Biomedical Engineering Letters (2019) 9:279–291
https://doi.org/10.1007/s13534-019-00122-y

REVIEW ARTICLE

Light sheet microscopy for histopathology applications

Praveen Kumar Poola[1] · Muhammad Imran Afzal[1] · Youngseung Yoo[1] · Ki Hean Kim[4] · Euiheon Chung[1,2,3]

Received: 25 February 2019 / Revised: 21 June 2019 / Accepted: 15 July 2019 / Published online: 24 July 2019

Abstract
Light sheet microscopy (LSM) is an evolving optical imaging technique with a plane illumination for optical sectioning and volumetric imaging spanning cell biology, embryology, and in vivo live imaging. Here, we focus on emerging biomedical applications of LSM for tissue samples. Decoupling of the light sheet illumination from detection enables high-speed and large field-of-view imaging with minimal photobleaching and phototoxicity. These unique characteristics of the LSM technique can be easily adapted and potentially replace conventional histopathological procedures. In this review, we cover LSM technology from its inception to its most advanced technology; in particular, we highlight the human histopathological imaging applications to demonstrate LSM's rapid diagnostic ability in comparison with conventional histopathological procedures. We anticipate that the LSM technique can become a useful three-dimensional imaging tool for assessing human biopsies in the near future.

Keywords Light sheet microscopy · 3D imaging · Tissue clearing · Histopathology · Clinical application

1 Introduction

Biopsies are of critical importance in medical diagnoses and tests to determine the presence or extent of disease [1, 2]. Conventional histopathological analyses of biopsies involve a tedious process of fixing and staining and thus the destruction of biopsy tissue [3–5]. Moreover, biopsy does not always provide sufficient information for accurate disease diagnosis due to biopsy sampling errors and disagreement regarding the diagnosis among pathologists when interpreting biopsy specimens [6–8]. The standard procedure for analyzing biopsies not only requires a lot of time and effort but can also lead to the degradation of nucleic acids [9, 10]. In addition, histopathological procedures consume the tissue to the extent that there might not be sufficient residual tissue for supplemental molecular studies, causing problems down the line if questions still remain [10, 11].

Moreover, in preparation for postoperative pathological evaluation, radical prostatectomy specimens are grossly processed by manually cutting the organ into cross-sectional slices of 3–5 mm in thickness, as shown in Fig. 1a [12, 13]. There are a number of nondestructive fluorescence microscopy methods for human biopsies, such as confocal microscopy [14, 15] and nonlinear microscopy [16–19]. However, the complex setup, high volume of photobleaching, slow acquisition speed, and three-dimensional (3D) raster scanning of small focal points have made these approaches inconvenient for clinical use. In the majority of traditional microscopes, the illumination and collection configurations are coupled, which places constraints on imaging performance; for instance, there is a trade-off between field of view and depth of focus. In contrast, in wide-field microscopy techniques, unnecessary excitation of out-of-focus fluorescence degrades the quality of the in-focus signal (Fig. 2). By decoupling the illumination and detection optics with a sheet of light, LSM provides fast wide-field imaging of three-dimensional samples without out-of-focus photobleaching.

In current clinical settings, there is an urgent need for wide-area, slide-free, fast, and nondestructive biopsy

✉ Euiheon Chung
ogong50@gist.ac.kr

1 Department of Biomedical Science and Engineering (BMSE), Gwangju Institute of Science and Technology (GIST), Gwangju 61005, Republic of Korea

2 Institute of Integrated Technology, GIST, Gwangju 61005, Republic of Korea

3 School of Mechanical Engineering, GIST, Gwangju 61005, Republic of Korea

4 Department of Mechanical Engineering, Pohang University of Science and Technology, 77 Cheongam-ro, Nam-gu, Pohang, Gyeongbuk 37673, Republic of Korea

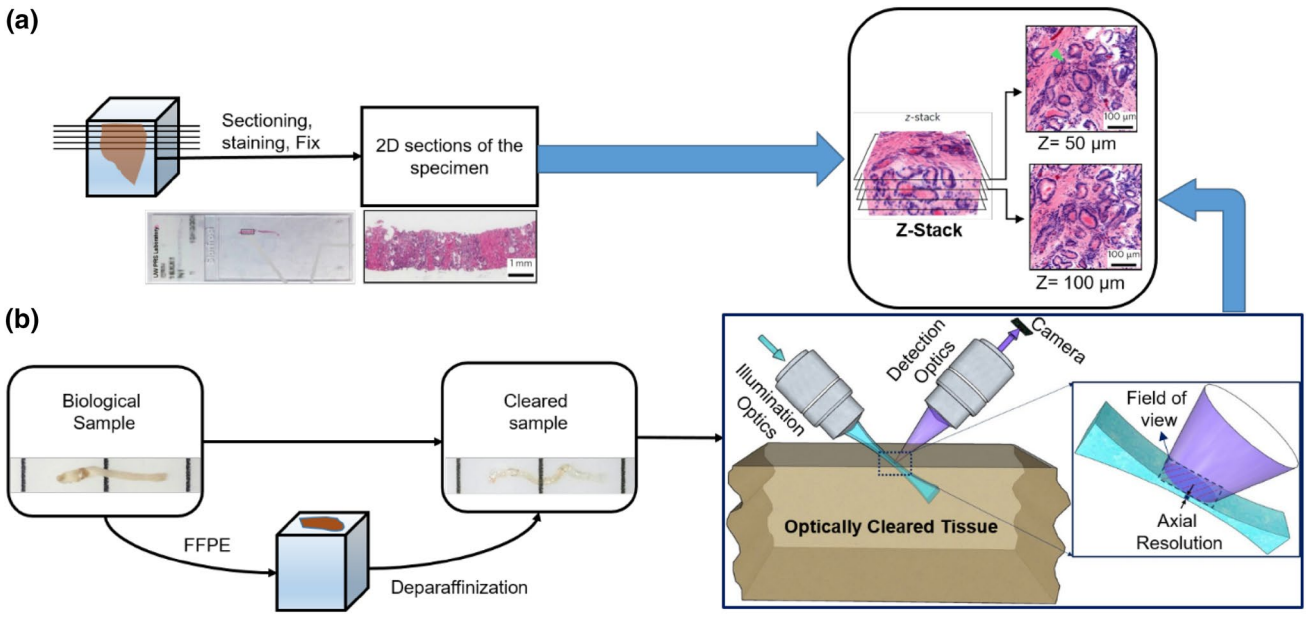

Fig. 1 Light sheet microscopy for biological specimens of unlimited size. Sweeping the light sheet (LS) in a perpendicular direction can generate rapid volumetric imaging. *FFPE* formalin-fixed paraffin-embedded. **a** Traditional histological procedure showing 2D slices by manual sectioning of the tissue specimen. **b** LSM tissue histological process showing the optical sectioning of the tissue

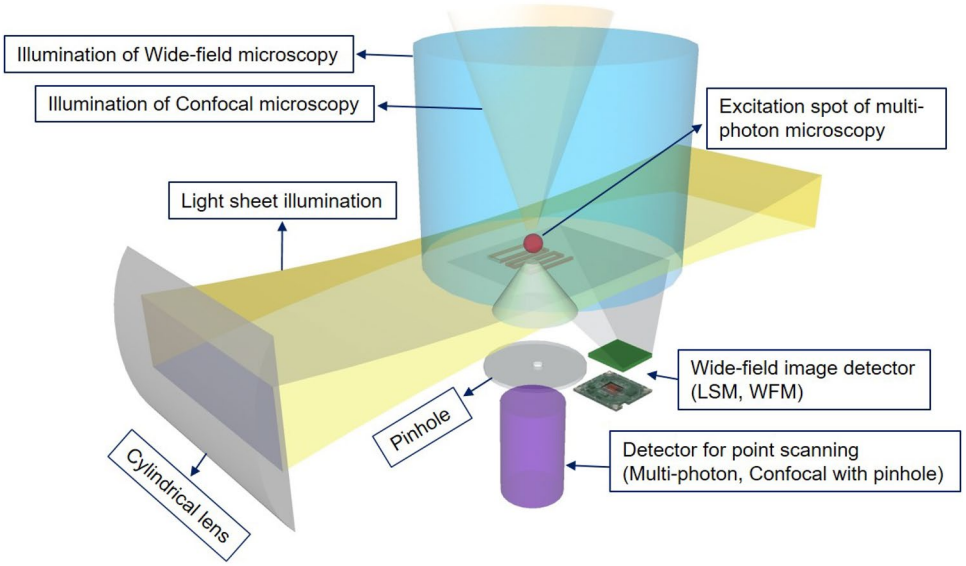

Fig. 2 Comparison of illumination shapes and detection schemes of various microscopy techniques

procedures. LSM has drawn the attention of clinical pathologists as its optical sectioning capability can provide 3D volumetric information without physically cutting the specimen [20–22]. The LSM technique can reduce the biopsy time from hours to minutes with imaging speed of 10–75 frames per second [23]. During the last decade, the LSM technique has contributed immensely to the fields of developmental biology [24, 25], embryology [21], neurobiology [26], drug discovery [27], plant biology [28], and oceanography [29].

The conventional histopathological procedure is shown in Fig. 1a. On the other hand, the LSM technique's histological procedure just requires an optically cleared sample to obtain volumetric 3D information of the specimen without physically cutting it, as described in Fig. 1b. Thus, LSM tissue histology has the potential to replace conventional histology. The principle of LSM stems from decoupling the illumination and detection optics, allows efficient collection of signal photons from the sheet illumination. The beam shaping optics to form a light sheet often includes a

cylindrical lens, slit apertures, and beam-expanding optics. In addition, combining the light sheet (LS) technology with a fast laser scanning mechanism, a rapidly scanning thin light sheet can be formed; this technique is named digital scanned laser light sheet fluorescence microscopy (DSLM) [21]. The detection is performed in a direction orthogonal to the illumination optics in order to maximize photon detection efficiency by minimizing the fluorescence from the out-of-focus plane [22]. LSM generates photons in the focal plane so as to minimize the wastage of photons from out-of-focus layers. Owing to the minimum background in the region of interest, it is possible to achieve a better SNR with lower light illumination power. The photobleaching is reduced by a factor of n, where n = number of optical sections. Various microscopy techniques, including LSM, are compared with their performance indicators, key applications, and main limitations, as summarized in Table 1.

2 History of light sheet microscopy

The original LSM technique termed "ultra-microscopy" was pioneered in 1902 by Richard Adolf Zsigmondy to observe colloidal gold particles by focusing sunlight, which was described in his Nobel lecture in 1925 [30]. For many years, the method was not used, until 1993 when Arne Voie developed orthogonal-plane fluorescence optical sectioning (OPFOS) microscopy [31] by combining planar illumination with fluorescence microscopy to image the inner ear cochlea of the guinea pig with a 10-µm lateral and 26-µm axial resolution over a 1.5 × 1.5 mm field of view (FOV). Despite the success of OPFOS, the LSM technique has remained obscure for several years. The breakthrough in LSM occurred with the invention of selective plane illumination microscopy (SPIM) by Ernst H. K. Stelzer's group in 2004 [32]. Although SPIM featured relatively minor technical differences compared with its predecessors, the real breakthrough occurred with its application to the in *vivo* imaging of transgenic GFP-expressing model organisms, including GFP-labeled muscle in the naturally transparent Medaka fish *Oryzias latipes* and embryogenesis of the common fruit fly *Drosophila melanogaster* using GFP-moesin (a plasma membrane marker).

2.1 Principles and practical implementation of light sheet microscopy

The primary requirement for LSM imaging is the need for a relatively clear sample. Ex vivo clearing of a sample can be performed by any one of a range of protocols [33]. Once the tissue has been cleared optically, we can proceed for imaging by placing the cleared tissue onto the microscope's stage. LSM's key feature is its ability to capture in-focus images of a wide area to a depth on the order of millimeters. The laser beam focuses into a thin sheet of light that excites only the fluorophores within it, producing an optical section ranging from 0.4 to 26 µm. Since the optical sectioning is a nondestructive process, it does not involve the physical cutting of tissue. In LSM, the illumination and detection optics are placed perpendicular to each other. The idea of using separate paths provides the flexibility to tune and optimize the light sheet thickness according to the required application; in other words, by tuning the LS thickness, we can change the resolution, FOV, and depth of focus of the imaging system. The whole sample is scanned using a laser LS for the 3D-volumetric image. This enables 3D imaging of tissues in rapid succession. Using this technique, we may complete the whole biopsy within minutes. By using post-processing

Table 1 Detailed parametric comparison of the different techniques

Technique	Wide-field microscopy	Confocal microscopy	Multiphoton microscopy	Light sheet microscopy
Standard spatial resolution	< 0.5 µm (lateral) and not applicable (axial)	< 0.4 µm (lateral) and < 2 µm (axial)	< 0.5 µm (lateral) and < 3 µm (axial)	< 0.5 µm (lateral) and < 3 µm (axial)
Imaging speed	High (area)	Slow (point scanning)	Slow (point scanning)	High* (volume scan)
Imaging depth	Limited	Limited	Best	Limited/high
Illumination shape	Wide-field and uniform illumination	Point illumination (hourglass shaped excitation)	Point illumination (nonlinear focal excitation)	Light sheet illumination (decoupled from detection)
Detection	Wide-field detector	Point detector	Point detector	Wide-field detector
Key application	Thin micro-slice 2D imaging	Very high-volumetric resolution	Deep tissue volume imaging	Fast volume imaging, transparent or optically cleared specimen
Main limitation	No axial resolution, photodamage	Imaging speed, imaging depth, and photodamage	Imaging speed and potential nonlinear photodamage	Imaging depth and inhomogeneity of image quality

*With the use of a faster scanning approach, such as resonant scanning, the speed can reach up to video rate at the cost of a low signal-to-background-noise ratio (SNR)

techniques, digital images can be pseudocolored to assimilate conventional hematoxylin and eosin (H&E)-stained sections [57]. The biopsy process using the LSM technique preserves the tissue to be used for later supplemental studies, which is an advantage over conventional methods. Having multiple advantages, the LSM technique has recently gained popularity in the fields of developmental biology and neuroscience [24, 25].

2.2 Essential LSM system requirements

For the LSM system, the first factor to be considered is the illumination optics. This allows uniform illumination across the sample FOV with good optical sectioning capability and allows the light to penetrate deep inside the tissue. In addition to the LSM optical design, depth of field, working distance, and FOV play important roles in selecting the illumination objective lens and detection objective lens. Depending on the type of specimen to be imaged, the illumination optics numerical aperture (NA) and magnification vary from 0.1 to 0.3 and 2× to 10×, respectively. In the case of detection optics, NA value varies from 0.2 to 1.1, which includes dipping or water immersion objectives with long working distances and allows steep angles. For particularly interested readers, greater detail on the basic optical system can be found in an earlier paper by Stelzer [32]. The LS has to travel into an inhomogeneous environment with properties of high scattering and absorption. Owing to the regions with a higher refractive index in the sample, the signal-to-background-noise ratio (SNR) is decreased due to aberrations [34, 35]. As a consequence, the optical path length increases, and the image quality deteriorates. There has been considerable interest in the optimization of illumination optics to minimize the scattering and absorption of light [34, 35] inside the tissue. Engineered beams, such as Bessel, airy, and lattice beams, were adapted to reduce the scattering and propagate the LS deep inside the tissue without diffraction [36–39]. Alternative methods to minimize the effects of scattering and absorption involved removing the chromophores from the tissue using chemical agents or tissue-clearing techniques [33, 62, 63].

After the illumination optics, the next factor to be considered is the sample mounting component. This allows a linear focal scan of the tissue to reconstruct the 3D volumetric image of the sample. To achieve this task, synchronization among the stage, LS, and camera is necessary. The use of an electrically tunable lens [40] is one of the efficient ways of axial scanning when compared with other axial scanning methods reported in the literature [20, 21, 32].

While the lateral resolution depends on the detection optics, the axial resolution can also be affected by the thickness of LS illumination. In addition, spherical and other optical aberrations will affect the final achievable resolution of the system [27, 34, 41]. There is a compromise between the effective NA of an objective lens and the geometry of the LS, including the central thickness and uniformity. Here, the effective NA means the resultant numerical aperture effectively employed by the illumination beam, which can differ from the objective NA.

2.3 Recent developments of LSM techniques

LSM stands out as an ideal technique to image 3D biological samples with features of low photobleaching, high spatiotemporal resolution, and high SNR [42]. Imaging large, living specimens with high resolution still remains challenging with the existing LSM system configurations. There are various LSM system configurations depending on the size of the sample and speed. In this section, we cover recently proposed developments in LSM configuration to overcome the above issues. Thanks to multiview reconstruction methods [24, 43, 44], the uniformity of the image quality is improved in strongly scattering and absorbing samples, whereas in transparent samples, the axial resolution is strongly enhanced to the point that the resolution becomes isotropic. The first SPIM setup was proposed by Huisken [32], in which the LS was generated inside a chamber filled with buffer solution. The tissue specimen was immersed in the buffer solution from the top so that it can be rotated in multiple directions. However, multiview reconstruction through the rotation of a sample comes with several disadvantages. First, owing to the difficulties in precise rotation of the axis with respect to the specimen, there is a need to realign the misaligned images using computational algorithms. Second, the artifacts coming from the biological dynamics are faster than the sample rotation speed. Finally, a longer sample exposure time is required for multiple views than with the basic LS microscope, which increases the photobleaching and phototoxic effects [43–45].

The need to collect high-SNR images of opaque specimens while retaining high temporal resolution and low phototoxicity has led to the development of dual excitation LSM [46]. The simpler solution is to add a third magnification objective lens to the existing dual LSM to illuminate the sample sequentially from two opposing directions, similar to that in multiview SPIM (mSPIM) [47, 48]. The requirement for fast image acquisition has led to the development of a MuVi-SPIM [43, 47] system with the addition of a second magnification objective lens to the detection arm. The total MuVi-SPIM system consists of four magnification objective lenses, two for illumination and another two for detection, arranged in a fixed geometry for multiview data fusion in real time. To increase the LS efficacy, both of the detection objective lenses are operated simultaneously and focused onto a common focal plane. However, the illumination objective lenses work alternately to avoid image

blurring due to the increased scattering coming from the two LSs simultaneously. Similar to the MuVi-SPIM system, SiMView [49] is a four-armed LS microscope with single-photon and multiphoton excitation. SiMView consists of automated software to ensure the perfect alignment of LSs and detection arms to increase the spatiotemporal resolution [50]. mSPIM, MuVi-SPIM, and SiMView systems have been used successfully to image dynamic biological events in *Drosophila melanogaster* embryos and live zebrafish in comparison with conventional SPIM [47]. In addition, Wu et al. have developed a new LSM technique with high isotropic spatial resolution [46]. The setup is built on a dual inverted SPIM (iSPIM) microscope [51, 52] consisting of two magnification objective lenses arranged orthogonally that are used alternately for illumination and detection. The technique retains the LSM system's advantages previously described in this section but has a faster acquisition speed with isotropic resolution. Recently, lattice light sheet microscopy (LLSM) from Eric Betzig's group has pushed the rapidly growing LSM field to the next level by offering fast and high-resolution imaging using a lattice of interfering Bessel beams [42]. Advanced techniques, such as LLSM, should find applications in characterizing the histology with its submicron resolution.

Swept confocally aligned planar excitation (SCAPE) [53] was proposed as an alternative technique to image samples using a single magnification objective lens in *en face* geometry. This geometry does not necessitate synchronization between the illumination and detection planes. Since it uses a single objective lens, sample geometry constraints are very minimal compared with those in other LSM geometries. However, the SCAPE microscope hinders the imaging of a larger volume of intact biological samples. Raju Tomer's [54] group has addressed this fundamental limitation of imaging large biological samples using light sheet theta microscopy (LSTM) by uniformly illuminating the sample at a particular angle to eliminate the limits on lateral dimensions without sacrificing the resolution, depth of field, and speed. SIM in combination with light-sheet-based fluorescence microscopy (csiLSFM) is a recently proposed method to enhance the lateral resolution down to below 100 nm [55]. This system uses three magnification objective lenses, where two objective lenses are used for generating the SIM patterns in the focal plane, which are flexibly rotated to provide the near-isotropic lateral resolution.

To summarize this section, we have tabulated the state of the LSM techniques and their relative merits, such as axial and lateral resolution and FOV, in Table 2.

3 Commercially available microscopes

For biomedical professionals to utilize LSM, some companies have commercialized LSM systems. We summarize the commercially available products below:

1. *Lightsheet Z.1* is the first commercialized LSM system from Zeiss. It is based on the setup introduced by Stelzer [32], and it is mainly designed for the multiview imaging of large, living specimens. This version of the LSM system is well suited for research in developmental biology and for following cellular dynamics in small model organisms.
2. *Luxendo* provides an alternative LSM system MuVi-SPIM microscope based on the setup developed by Krzic [44, 47]. The MuVi-SPIM system has four orthogonal views of the sample that works without rotation. This version of the LSM system has a high acquisition speed, long-term sample stability, and data fusion precision. It is typically applied to small animal models and mammalian cell culture for 3D reconstruction and the tracking of cellular and sub-cellular positions.

Table 2 State-of-the-art LSM technology and associated imaging parameters

Technique	Lateral resolution (μm)	Axial resolution (μm)	Field of view
Ultra microscopy [orthogonal-plane fluorescence Optical o sectioning (OPFOS)]	10	26	1.5 mm (FOV)
Thin light sheet microscopy (2002)	10	23	1 mm (FOV)
Selective plane illumination microscopy (SPIM) (2004)	1	3–10	1.5×0.9 mm^2
SCAPE	0.4–2	0.5–3	$0.6 \times 1 \times 0.55$ mm^3
Open-top LSM	1.4	7	$3.3 \times 3.3 \times 1.28$ mm^3 (4× objective lens) (optically cleared human biopsy specimen)
Light sheet theta microscopy (LSTM)	0.4–2	2–5	$1.3 \times 1.3 \times 3$ mm^3 (10× objective lens) (optically cleared human brain tissue)

3. *LaVision BioTec* introduced an UltraMicroscope II LSM system based on the design of Hans-Ulrich Dodt [20]. This bidirectional LSFM generates stripes and artifact-free data at a very fast speed (100 fps at full frame) using six light sheets (three from each side with different angles). This system has been successfully demonstrated on neurobiology applications and to study neovascularization and lymph nodes, as well as developmental steps in animal models at cellular resolution.
4. *3i (Intelligent Imaging Innovations)* provides a lattice LS microscope with a uniform LS of submicrometer thickness based on the setup developed by Eric Betzig [42]. The creation of a lattice Bessel beam generates a 0.4-μm-thick LS that extends to 50 μm, which allows the collection of images at 100–500 fps using a high-speed CMOS camera. It is thus possible to observe cell–cell interaction, single-molecule diffusion into spheroids, as well as cell motility in a 3D matrix and embryogenesis with high spatial and temporal resolution. It supports conventional sample holders, such as coverslips and Petri dishes, as well as custom-designed chambers. Thus, it is adapted to image specimens of various sizes ranging from single cells to whole organisms.
5. *Leica* has commercialized the TCS SP8 DLS (digital LS) microscope with the addition of a TwinFlect mirror device to deflect the LS at a 90° angle to a commercial confocal microscope. In the approach chosen by Leica, they made use of two opposing 45° mirrors that are attached to the condenser lens of the illumination arm. By reflecting and rapidly scanning the laser light coming from the diascopic (transmitting illumination) arm, a LS is formed in the sample and imaging is performed through the microscope's objective lens [21]. It is mostly used to observe embryogenesis and developmental processes of embryos at a maximum speed of 60 fps.
6. *Phase View* designed an Alpha3 microscope that can reach 100 fps at full frame with their CMOS camera. The sample is left stationary. It can perform high-speed volumetric imaging of weakly fluorescent specimens as well as live imaging of 3D cell cultures.

Apart from buying a ready-made microscope, it is also possible to build a basic LSM according to detailed instructions (http://openspim.org), and the list of parts is available for the LSM setup. This integrated Open-SPIM hardware and software platform is an open-access initiative for building and adapting SPIM technologies [56]. The idea is to make SPIM technology available to the broad scientific community, including those without an optics background. Instructions are provided with pictures that show the step-by-step building procedures. In addition, an OpenSPIM/Fiji software package is available with tutorials to program and modify the source code. The simplest setup fits on an optical breadboard of 30 × 45 cm. It is developed mainly for studies of development, such as embryogenesis. Videos are made available with instructions on how to build the setup and align the microscope properly.

4 Light sheet microscopy (LSM) for histology imaging

To meet pathologist's demands for analyses of fresh tissue and to examine tissues in rapid succession, Jonathan Liu's group from the University of Washington developed open-top light sheet microscopy by adapting a previously developed LSM technology [57]. This newly developed nondestructive OT-LSM was demonstrated on large fresh human biopsy samples extracted from breast, prostate, and kidney tissues. This demonstration highlighted the LSM technique as a promising histopathological tool to image large human samples within tens of minutes. In addition, the OT-LSM images are comparable to standard histology images. This confers an advantage of sampling biopsies digitally rather than separating them into tiny fractions. OT-LSM's volumetric imaging of tissue can improve pathologists' ability to diagnose diseases and stage lesions. The technique currently offers cellular resolution, but over extensive areas without tissue damage and potentially with much less nucleic acid degradation. This OT-LSM technique was also demonstrated for rapid evaluation of surgical specimen margins during surgery.

In the next section, we have discussed the potential transformative diagnostic paradigm of LSM for several selected clinical applications, with a special emphasis on human histology.

4.1 Human prostate tissue

OT-LSM was explored in the postoperative evaluation and triage of large surgical resection specimens, for which optically cleared prostate tissue was considered. An optical image of fresh prostate tissue is shown in Fig. 3a, and its corresponding OT-LSM histological image is shown in Fig. 3b. An *en face* surface image is shown at the top left of Fig. 3b before applying the surface extraction algorithm on a 3D volumetric dataset to show the regions of defocus and incomplete imaging. The bottom right of Fig. 3b shows the irregular surface of the large specimen after applying the digital surface extraction algorithm. From Fig. 4a, we can observe both basal and epithelial cells from the normal prostate glands. Specifically, we can observe a tissue transformation from benign to adenocarcinoma status at the cellular level from Fig. 4b as evidenced by the crowding of glands with a single epithelial cell layer. Figure 4c displays neoplasia stratified nuclei in a lumen. All of the images were

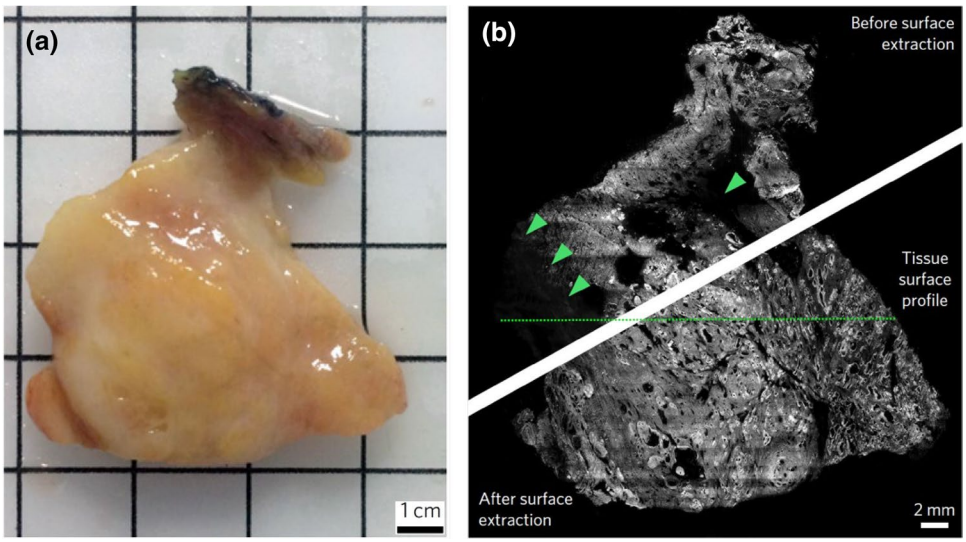

Fig. 3 **a** An optical image of fresh human prostate tissue (3.1 × 3.5 × 0.4 cm). **b** OT-LSM histological image before and after applying the surface extraction algorithm. Surface extraction is a form of digital image processing to provide a comprehensive image of the surface to compensate for the irregular surface of the large specimen from the 3D dataset as there are defocused and incomplete regions in the original image (arrowheads). All images were reproduced with permission from Ref. [57]

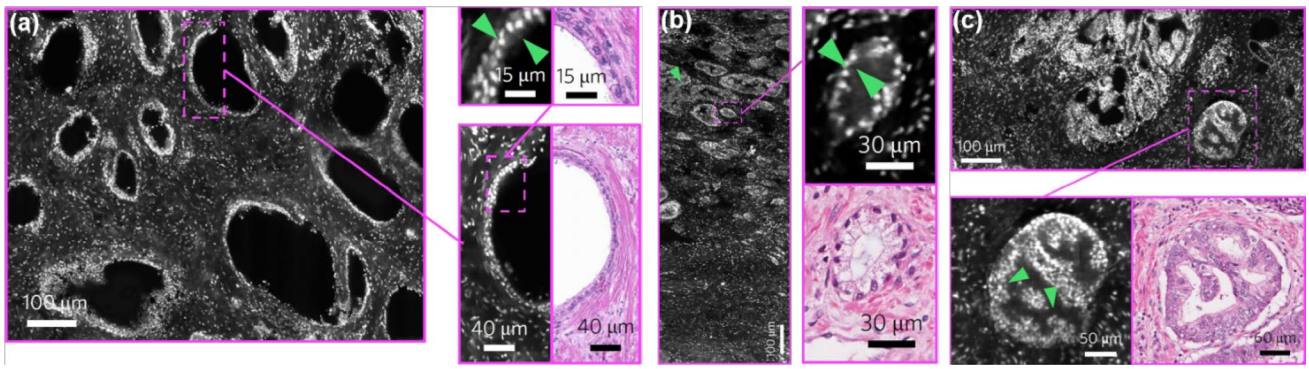

Fig. 4 **a** Moderate- and high-magnification images of normal prostate glands, where a layer of both basal and epithelial cells is observed (arrowheads). A corresponding H&E histological image is shown on the right. **b** A region with benign prostate (left) transitioning into prostate adenocarcinoma (right), which exhibits the crowding of glands with a single epithelial cell layer (arrowheads). A corresponding H&E histological image is shown in the lower panel. **c** High-grade prostate intraepithelial neoplasia, displaying stratified nuclei and tufted projections into the lumen (arrowheads). A corresponding H&E histological image is shown on the right. All images were reproduced with permission from Ref. [57]

supplemented with corresponding H&E histology images shown alongside.

OT-LSM was explored for intraoperative imaging of large freshly resected human breast tissue composed of a pliable adipose specimen for tumor margin assessment. Figure 5a shows the biopsy tissue, and Fig. 5b shows the conventional histology image of the corresponding specimen. It is evident from Fig. 5c that the LSM technique could reveal structural details of an optically uncleared specimen. The LSM comprehensively images benign fibro-adipose tissue at a quality comparable with that of conventional archival formalin-fixed paraffin-embedded (FFPE) histology. The imaging time is less than 1 min to extract the OT-LSM histological image after surface extraction. A digital surface extraction algorithm was used to obtain the entire tissue surface from the raw 3D dataset.

Human breast imaging was also performed using a multimodal approach by combining ultrasound, photoacoustic tomography, and inverse SPIM (iSPIM). The iSPIM result in Fig. 6a shows the maximum intensity projection of a stack representing the anterior surface of the breast sample showing cell types and nuclear features. The stromal features of fatty tissue are presented in Fig. 6b, d, whereas micro-calcifications and small vessels are visible in Fig. 6c, e, respectively. All of the results are correlated with the histology results.

4.2 Human brain imaging

To image large biopsy samples, Raju Tomer's group from Columbia University developed LSTM [54]. LSTM was demonstrated on human brain sections of

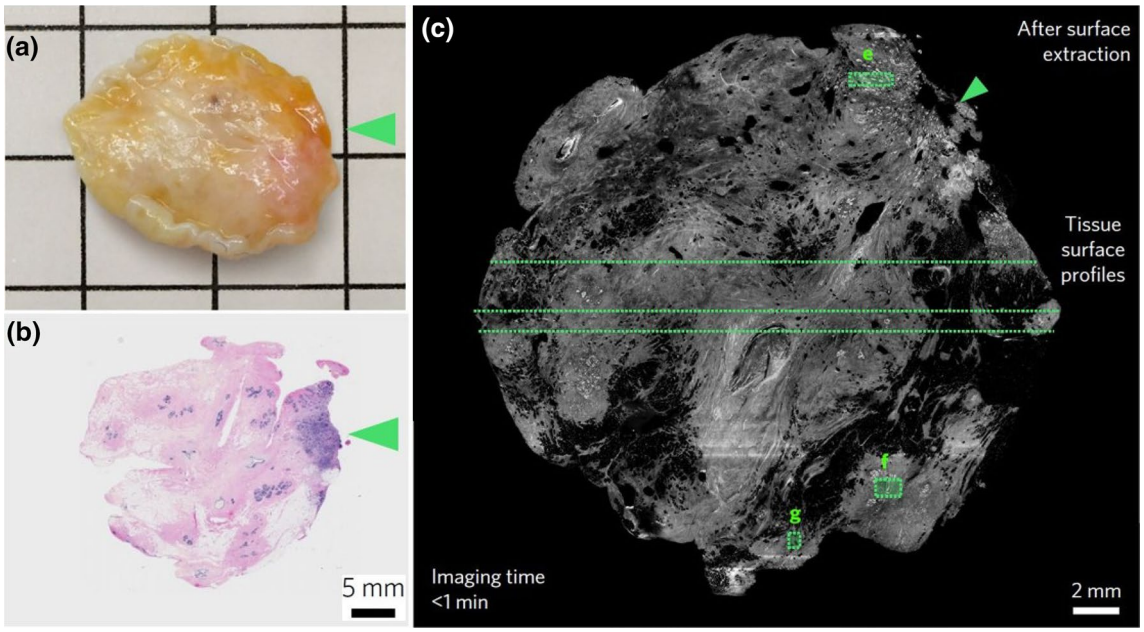

Fig. 5 Human breast tissue. **a** A freshly excised specimen of human breast tissue (2.0×2.0×0.4 cm). **b** Conventional histological image of the corresponding specimen. **c** Open-top light sheet microscopy of human breast tissue; the arrowheads indicate a region of invasive carcinoma (i.e., a positive margin). All images were reproduced with permission from Ref. [57]

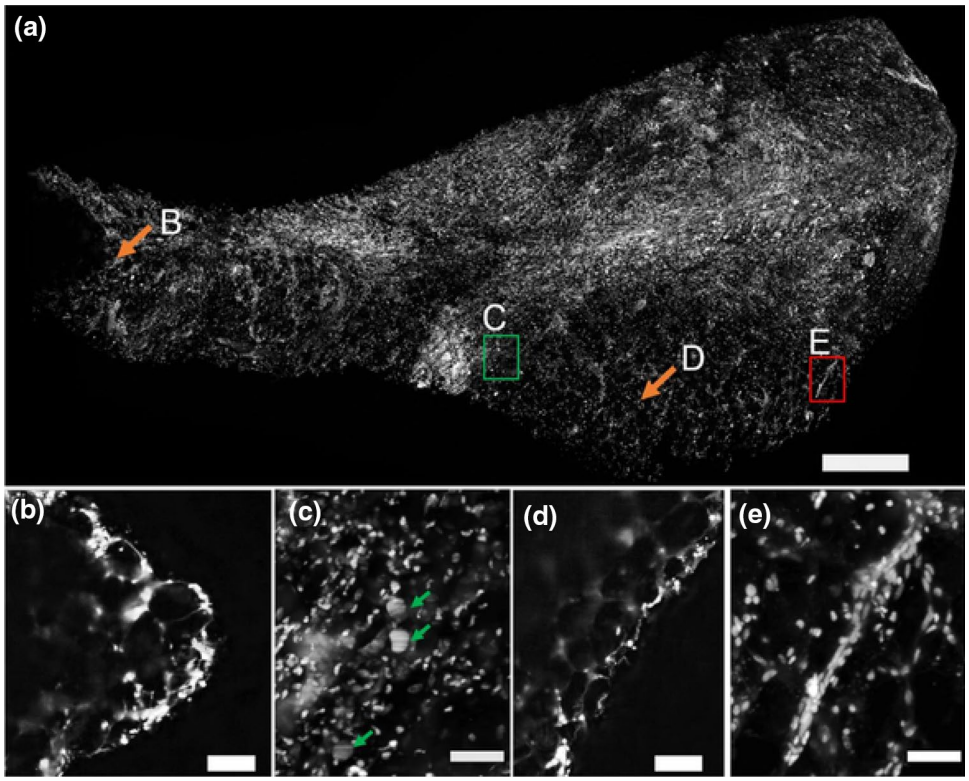

Fig. 6 **a** Representing the anterior side of the biopsy. **b**, **d** Various structures, such as fatty tissues. **c** Micro-calcifications (green arrows) and **e** small blood vessels. The arrows and the boxes in a indicate the sites of the lower-magnification images in the biopsy. Scale bars in **a**: 500 µm, in **b**, **d**: 100 µm, and in **c**, **e**: 50 µm. All images were reproduced with permission from Ref. [59]. (Color figure online)

~ 10.5 × 14.1 × 3 mm in size. Figure 7 shows an LSTM image of a human brain sample stained with DAPI. This result is the first of its kind to report on the human brain using LSM.

4.3 Human gingiva imaging

The LSM technique was also demonstrated to be promising for characterizing human gingival morphology and

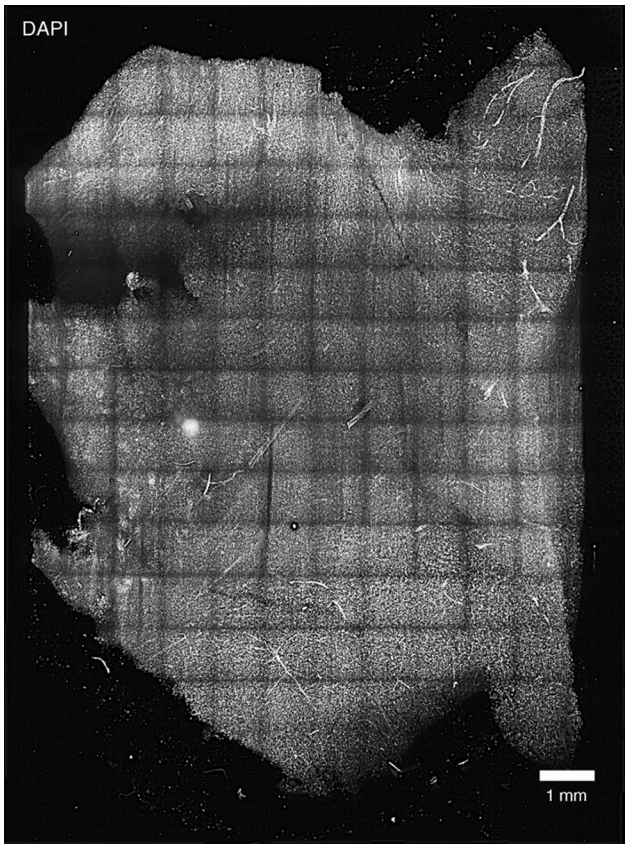

Fig. 7 LSTM imaging of a large thick section of cleared human brain tissue (~ 10.5 × 14.1 × 3 mm) stained with DAPI. Scale bar is 1 mm. All images were reproduced with permission from Ref. [54]

vasculature from a patient's waste material. The 3D images of capillary loops in stromal papillae invading into the stratified epithelium of human gingiva as shown in Fig. 8a prove the potential of LSM in oral health and disease diagnostics. Figure 8b is a stack of sections of stromal papillae prepared based on Fig. 8a. The tortuosity and irregular shape of the capillary loops are clearly visible in Fig. 8c but are not apparent in 2D images of conventional procedures, such as periodic acid–Schiff (PAS) (Fig. 8d) and Giemsa staining (Fig. 8e, f). This indicates the relevance of LSM in 3D histochemistry and imaging of healthy and pathological human gingival samples.

4.4 Human temporal bones imaging

At present, µCT is used to evaluate the middle and inner ear temporal bone features, but using µCT, it is difficult to see the morphology of human soft bones. To bridge this gap, thin-sheet laser imaging microscopy (TSLIM) was used to image the morphology of human temporal bone (cochlea) instead of traditional celloidin sectioning [60]. The results of this study have revealed the structures of spiral ligament, stria vascularis, Reissner's membrane, and organ of Corti. Figure 9a shows the TSLIM image of the basal turn cross section of the right temporal bone (TB), whereas Fig. 9b shows the processed TSLIM image of the basal turn celloidin cross section. To correlate TSLIM results with the histology, an H&E-stained image is shown in Fig. 9c.

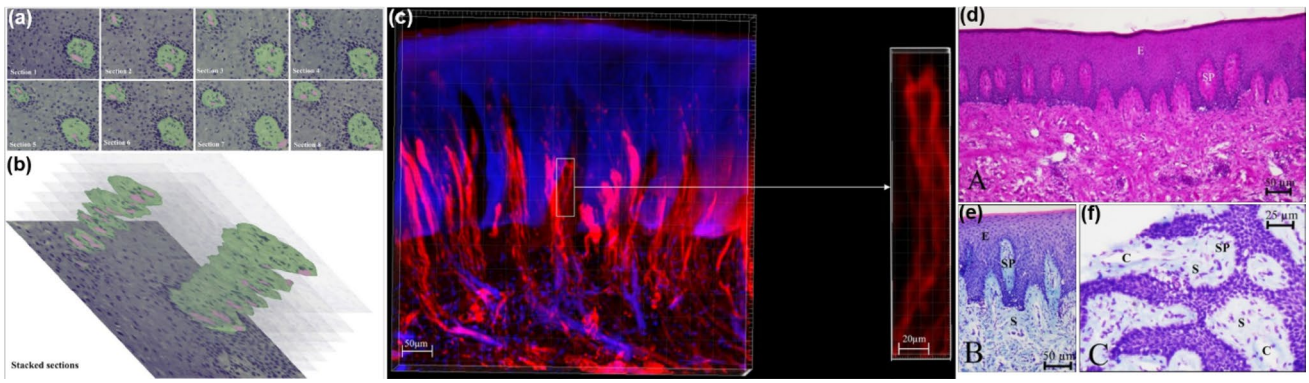

Fig. 8 **a** Serial cryostat sections (8 µm thickness) after staining with hematoxylin of gingival epithelium (blue) invaded by stromal papillae (green) containing ascending and descending limbs of a capillary loop (pink) after the BABB clearing procedure. **b** Stacks of sections of stromal papillae prepared based on the images in (**a**; A). Epithelium is shown as in Sect. 1. One papilla is sectioned from the top toward the bottom (upper papilla), and the other is sectioned halfway to the bottom. **c** Low-magnification 2D projection of a 3D image prepared with the use of light sheet microscopy of human gingiva embedded in agarose with the endothelium of blood vessels immunohistochemically stained using anti-CD31 antibodies conjugated with Alexa Fluor 568 (red) and nuclear staining using YOYO-3 (blue). Note that pseudocolors are used to optimize contrast. Detailed image bar of a capillary loop (red) in a connective tissue papilla that is invading into the epithelium of human gingiva in the box was taken from the 3D image. Bar = 20 µm. **d** Light microscopy images of cryostat sections of the gingival sample stained with PAS. **e**, **f** Giemsa staining regions marked with E, S, and SP on (**e**, **f**) are staining of the epithelium (E), stroma (S), and stromal papillae (SP) containing capillaries. Bars = 50 µm (**d**, **e**) and 25 µm (**f**). All images were reproduced with permission from Ref. [58]. (Color figure online)

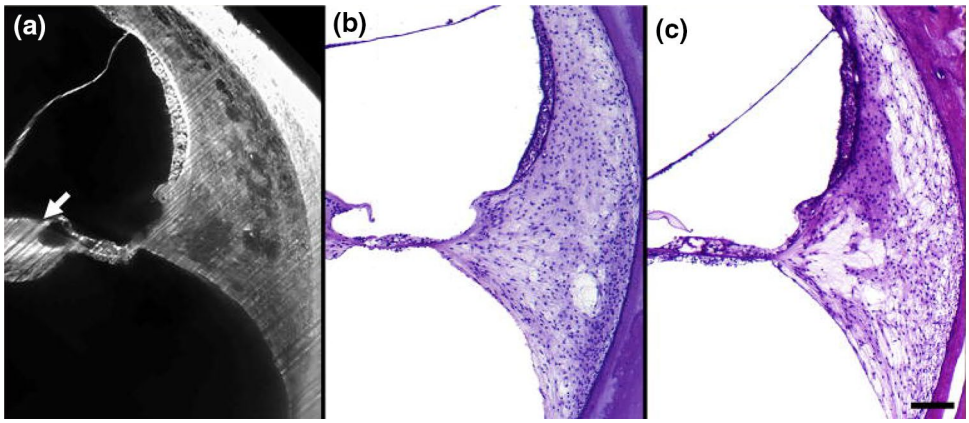

Fig. 9 **a** High-magnification basal turn cross section of the right temporal bone (TB) showing absorption artifacts (dark lines at arrow). **b** High-magnification basal turn celloidin cross section of the TSLIM-processed right TB. Reissner's membrane became detached from the spiral limbus in the right TB (panels **a** and **b**). **c** H&E-stained, high-magnification basal turn celloidin cross section of the left TB. Bar = 100 µm. All images were reproduced with permission from Ref. [60]

4.5 Human skin imaging

The last application presented in this article is skin imaging using LSM, in SPIM in particular. Human skin biopsies of 5 mm in size are performed using LSM after making the human skin biopsies transparent using Murray's optical clearing. The LSM results show the different layers of the human skin, as shown in Fig. 10a, c. Figure 10b shows the H&E-stained normal skin, whereas Fig. 10d shows the H&E-stained pathological skin. * in Fig. 10a–d indicates epidermis, ** indicates papillary dermis, and *** indicates reticular dermis. The authors [61] in their article also showed autofluorescence of human skin from optically cleared specimens at several wavelengths (405, 488, 561, and 642 nm). The autofluorescence results are useful for identifying various skin layers, such as stratum corneum, dermis, and epidermal appendages. The results from the LSM are useful for visualizing and quantifying anomalies, such as epidermal hyperplasia from psoriasiform skin lesions.

5 Future directions and conclusions

The highly versatile LSM and its applications as presented in this article suggest the potential for using LSM techniques in clinical pathology settings. In this article, we mainly focused on the applications of LSM techniques in human biopsy; each of the applications in this article shows the results in comparison with the gold-standard histopathology. We have listed the significant advantages of the LSM technique over the traditional histological methods. We have also included the LSM's high speed and nondestructive 3D volumetric imaging to reduce the biopsy time. From the LSM applications discussed in this review article, we believe that using LSM can improve conventional histological processes in many cases.

The new developments, such as lattice LSM, can potentially increase the imaging speed and achieve lower phototoxicity, allowing in vivo live imaging. We expect that this LSM could find applications in biopsies, molecular testing, and intraoperative consultations. In the near future, the LSM technique could change the traditional biopsy procedures by offering pathologists 3D volumetric information with minimal sample preparation. Alternatively, the LSM technique could guide tumor surgery, providing an additional tool for pathologists for accurate disease diagnosis. The main future work could be adapting LSM in clinical settings, for which the need to add data visualization and computer-based analysis to the existing LSM technique will be a future direction to quickly make accurate tissue diagnoses from massive 3D datasets of LSM.

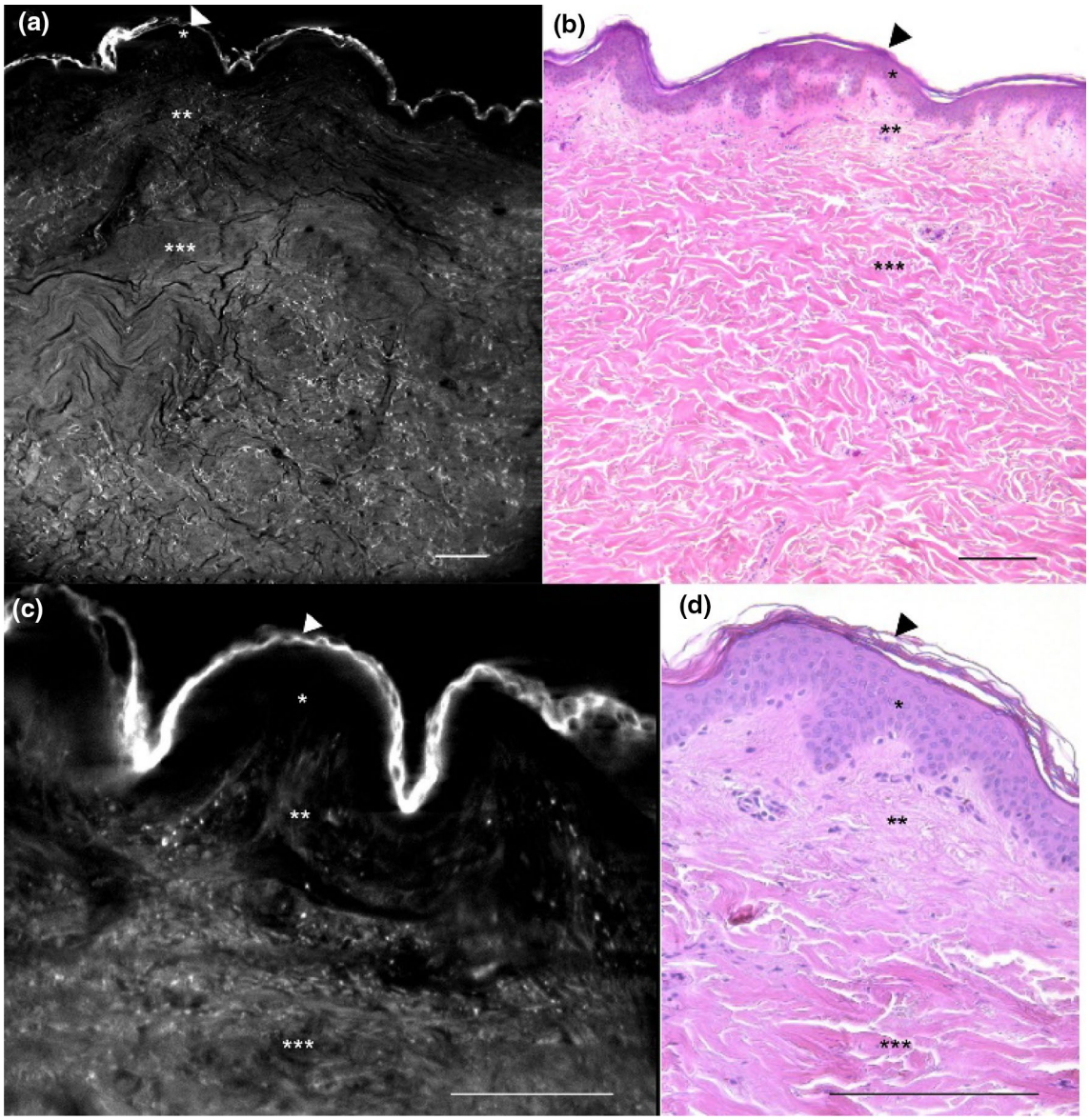

Fig. 10 Human skin structure was observed **a**, **c** on an optical cross section (slice at depth of 270 μm) by LFM and **b**, **d** using H&E staining. Arrowhead: stratum corneum; *epidermis; **papillary dermis; ***reticular dermis. Scale bars: 200 μm. All images were reproduced with permission from Ref. [61]

Acknowledgements This research was supported by a GIST Research Institute grant funded by GIST in 2019 and grants from the National Research Foundation of Korea (NRF) funded by the Korean government (MEST) (NRF-2016R1A2B4015381), by the Brain Research Program through the NRF funded by the Ministry of Science, ICT & Future Planning (NRF-2017M3C7A1044964), and also by the Bio & Medical Technology Development Program of NRF funded by the Korean government (MSIT) (NRF-2015M3A9E2030125). The authors thank Mr. Ripon Kumar Saha for preparing schematic drawings.

Compliance with ethical standards

Conflict of interest All authors declare that they have no conflicts of interest.

Ethical approval This work did not involve any studies with human participants or animals performed by any of the authors.

References

1. Eichler K, Hempel S, Wilby J, Myers L, Bachmann LM, Kleijnen J. Diagnostic value of systematic biopsy methods in the investigation of prostate cancer: a systematic review. J Urol. 2006;175:1605–12.
2. Hunninghake GW, Zimmerman MB, Schwartz DA, King TE Jr, Lynch J, Hegele R, Waldron J, Colby T, Müller N, Lynch D, Galvin J, Gross B, Hogg J, Toews G, Helmers R, Cooper JAD Jr, Baughman R, Strange C, Millard M. Utility of a lung biopsy for the diagnosis of idiopathic pulmonary fibrosis. Am J Respir Crit Care Med. 2001;164:193–6.
3. Gillett CE, Springall RJ, Barnes DM, Hanby AM. Multiple tissue core arrays in histopathology research: a validation study. J Pathol. 2000;192:549–53.
4. Pasyk KA, Argenta LC, Austad ED. Histopathology of human expanded tissue. Clin Plast Surg. 1987;14:435–45.
5. Tryka AF, Brooks JR. Histopathology in the evaluation of total pancreatectomy for ductal carcinoma. Ann Surg. 1979;190:373.
6. Berlin L. Accuracy of diagnostic procedures: Has it improved over the past five decades? AJR Am J Roentgenol. 2007;188:1173–8.
7. Hodel S, Laux C, Farei-Campagna J, Götschi T, Bode-Lesniewska B, Müller DA. The impact of biopsy sampling errors and the quality of surgical margins on local recurrence and survival in chondrosarcoma. Cancer Manag Res. 2018;10:3765.
8. Elmore JG, Longton GM, Carney PA, Geller BM, Onega T, Tosteson AN, Nelson HD, Pepe MS, Allison KH, Schnitt SJ, O'malley FP, Weaver DL. Diagnostic concordance among pathologists interpreting breast biopsy specimens. JAMA. 2015;313:1122–32.
9. Hewitt SM, Lewis FA, Cao Y, Conrad RC, Cronin M, Danenberg KD, Goralski TJ, Langmore JP, Raja RG, Williams PM, Palma JF, Warrington JA. Tissue handling and specimen preparation in surgical pathology: issues concerning the recovery of nucleic acids from formalin-fixed, paraffin-embedded tissue. Arch Pathol Lab Med. 2008;132:1929–35.
10. Srinivasan M, Sedmak D, Jewell S. Effect of fixatives and tissue processing on the content and integrity of nucleic acids. Am J Pathol. 2002;161:1961–71.
11. Xie R, Chung JY, Ylaya K, Williams RL, Guerrero N, Nakatsuka N, Badie C, Hewitt SM. Factors influencing the degradation of archival formalin-fixed paraffin-embedded tissue sections. J Histochem Cytochem. 2011;59:356–65.
12. Ohori M, Wheeler TM, Kattan MW, Goto Y, Scardino PT. Prognostic significance of positive surgical margins in radical prostatectomy specimens. J Urol. 1995;154:1818–24.
13. Eastham JA, Kattan MW, Riedel E, Begg CB, Wheeler TM, Gerigk C, Gonen M, Reuter V, Scardino PT. Variations among individual surgeons in the rate of positive surgical margins in radical prostatectomy specimens. J Urol. 2003;170:2292–5.
14. Masters BR, So PT, Gratton E. Multiphoton excitation microscopy of in vivo human skin: functional and morphological optical biopsy based on three-dimensional imaging, lifetime measurements and fluorescence spectroscopya. Ann N Y Acad Sci. 1998;838:58–67.
15. Rajadhyaksha M, Anderson RR, Webb RH. Video-rate confocal scanning laser microscope for imaging human tissues in vivo. Appl Opt. 1999;38:2105–15.
16. Masters BR, So PT. Confocal microscopy and multi-photon excitation microscopy of human skin in vivo. Opt Express. 2001;8:2–10.
17. Masters BR, So PT, Gratton E. Multiphoton excitation fluorescence microscopy and spectroscopy of in vivo human skin. Biophys J. 1997;72:2405–12.
18. Adur JF, Pelegati VB, Costa LF, de Thomaz AA, Almeida DB, Cesar CL, Pietro L, Andrade LA, Bottcher-Luiz F. Recognition of serous ovarian tumors in human samples by multimodal nonlinear optical microscopy. J Biomed Opt. 2011;16:096017.
19. Jain M, Robinson BD, Scherr DS, Sterling J, Lee MM, Wysock J, Rubin MA, Maxfield FR, Zipfel WR, Webb WW, Mukherjee S. Multiphoton microscopy in the evaluation of human bladder biopsies. Arch Pathol Lab Med. 2012;136:517–26.
20. Dodt HU, Leischner U, Schierloh A, Jährling N, Mauch CP, Deininger K, Deussing JM, Eder M, Zieglgänsberger W, Becker K. Ultramicroscopy: three-dimensional visualization of neuronal networks in the whole mouse brain. Nat Methods. 2007;4:331.
21. Keller PJ, Schmidt AD, Wittbrodt J, Stelzer EH. Reconstruction of zebrafish early embryonic development by scanned light sheet microscopy. Science. 2008;322:1065–9.
22. Olarte OE, Andilla J, Gualda EJ, Loza-Alvarez P. Light-sheet microscopy: a tutorial. Adv Opt Photonics. 2018;10:111–79.
23. Schmid B, Shah G, Scherf N, Weber M, Thierbach K, Campos CP, Roeder I, Aanstad P, Huisken J. High-speed panoramic light-sheet microscopy reveals global endodermal cell dynamics. Nat Commun. 2013;4:2207.
24. Weber M, Huisken J. Light sheet microscopy for real-time developmental biology. Curr Opin Genet Dev. 2011;21:566–72.
25. Stelzer EH. Light-sheet fluorescence microscopy for quantitative biology. Nat Methods. 2015;12:23–6.
26. Keller PJ, Dodt HU. Light sheet microscopy of living or cleared specimens. Curr Opin Neurobiol. 2012;22:138–43.
27. Verveer PJ, Swoger J, Pampaloni F, Greger K, Marcello M, Stelzer EH. High-resolution three-dimensional imaging of large specimens with light sheet-based microscopy. Nat Methods. 2007;4:311.
28. Maizel A, von Wangenheim D, Federici F, Haseloff J, Stelzer EH. High-resolution live imaging of plant growth in near physiological bright conditions using light sheet fluorescence microscopy. Plant J. 2011;68:377–85.
29. Fuchs E, Jaffe JS, Long RA, Azam F. Thin laser light sheet microscope for microbial oceanography. Opt Express. 2002;10:145–54.
30. Zsigmondy R. Colloids and the ultramicroscope: a manual of colloid chemistry and ultramicroscopy. New York: Wiley; 1909.
31. Voie AH, Burns DH, Spelman FA. Orthogonal-plane fluorescence optical sectioning: three-dimensional imaging of macroscopic biological specimens. J Microsc. 1993;170:229–36.
32. Huisken J, Swoger J, Del Bene F, Wittbrodt J, Stelzer EH. Optical sectioning deep inside live embryos by selective plane illumination microscopy. Science. 2004;305:1007–9.
33. Wan P, Zhu J, Xu J, Li Y, Yu T, Zhu D. Evaluation of seven optical clearing methods in mouse brain. Neurophotonics. 2018;5:035007.
34. Power RM, Huisken J. A guide to light-sheet fluorescence microscopy for multiscale imaging. Nat Methods. 2017;14:360.
35. Planchon TA, Gao L, Milkie DE, Davidson MW, Galbraith JA, Galbraith CG, Betzig E. Rapid three-dimensional isotropic imaging of living cells using Bessel beam plane illumination. Nat Methods. 2011;8:417.
36. Fahrbach FO, Gurchenkov V, Alessandri K, Nassoy P, Rohrbach A. Light-sheet microscopy in thick media using scanned Bessel beams and two-photon fluorescence excitation. Opt Express. 2013;21:13824–39.
37. Vettenburg T, Dalgarno HI, Nylk J, Coll-Lladó C, Ferrier DE, Čižmár T, Gunn-Moore FJ, Dholakia K. Light-sheet microscopy using an Airy beam. Nat Methods. 2014;11:541.
38. Fahrbach FO, Rohrbach A. Propagation stability of self-reconstructing Bessel beams enables contrast-enhanced imaging in thick media. Nat commun. 2012;3:632.

39. Truong TV, Supatto W, Koos DS, Choi JM, Fraser SE. Deep and fast live imaging with two-photon scanned light-sheet microscopy. Nat Methods. 2011;8:757.
40. Fahrbach FO, Voigt FF, Schmid B, Helmchen F, Huisken J. Rapid 3D light-sheet microscopy with a tunable lens. Opt Express. 2013;21:21010–26.
41. Tomer R, Lovett-Barron M, Kauvar I, Andalman A, Burns VM, Sankaran S, Grosenick L, Broxton M, Yang S, Deisseroth K. SPED light sheet microscopy: fast mapping of biological system structure and function. Cell. 2015;163:1796–806.
42. Chen BC, Legant WR, Wang K, Shao L, Milkie DE, Davidson MW, Janetopoulos C, Wu XS, Hammer JA III, Liu Z, English BP, Kiyosue YM, Romero DP, Ritter AT, Schwartz JL, Laylin LF, Mullins RD, Mitchell DM, Bembenek JN, Reymann AC, Böhme R, Grill SW, Wang JT, Seydoux G, Tulu US, Kiehart DP, Betzig E. Lattice light-sheet microscopy: imaging molecules to embryos at high spatiotemporal resolution. Science. 2014;346:1257998.
43. Tomer R, Khairy K, Amat F, Keller PJ. Quantitative high-speed imaging of entire developing embryos with simultaneous multiview light-sheet microscopy. Nat Methods. 2012;9:755.
44. Krzic U, Gunther S, Saunders TE, Streichan SJ, Hufnagel L. Multiview light-sheet microscope for rapid in toto imaging. Nat Methods. 2012;9:730.
45. Ahrens MB, Orger MB, Robson DN, Li JM, Keller PJ. Whole-brain functional imaging at cellular resolution using light-sheet microscopy. Nat Methods. 2013;10:413.
46. Wu Y, Wawrzusin P, Senseney J, Fischer RS, Christensen R, Santella A, York AG, Winter PW, Waterman CM, Bao Z, Colón-Ramos DA, McAuliffe M, Shroff H. Spatially isotropic four-dimensional imaging with dual-view plane illumination microscopy. Nat Biotechnol. 2013;31:1032.
47. Krzic U, Gunther S, Saunders TE, Streichan SJ, Hufnagel L. Multiview light-sheet microscope for rapid in toto imaging. Nat Methods. 2012;9:730.
48. Keller PJ, Ahrens MB. Visualizing whole-brain activity and development at the single-cell level using light-sheet microscopy. Neuron. 2015;85:462–83.
49. Royer LA, Lemon WC, Chhetri RK, Wan Y, Coleman M, Myers EW, Keller PJ. Adaptive light-sheet microscopy for long-term, high-resolution imaging in living organisms. Nat Biotechnol. 2016;34:1267.
50. Amat F, Höckendorf B, Wan Y, Lemon WC, McDole K, Keller PJ. Efficient processing and analysis of large-scale light-sheet microscopy data. Nat Protoc. 2015;10:1679.
51. Wu Y, Ghitani A, Christensen R, Santella A, Du Z, Rondeau G, Bao Z, Ramos DC, Shroff H. Inverted selective plane illumination microscopy (iSPIM) enables coupled cell identity lineaging and neurodevelopmental imaging in Caenorhabditis elegans. Proc Natl Acad Sci. 2011;108(43):17708.
52. Kumar A, Wu Y, Christensen R, Chandris P, Gandler W, McCreedy E, Bokinsky A, Colón-Ramos DA, Bao Z, McAuliffe M, Rondeau G, Shroff H. Dual-view plane illumination microscopy for rapid and spatially isotropic imaging. Nat Protoc. 2014;9:2555.
53. Bouchard MB, Voleti V, Mendes CS, Lacefield C, Grueber WB, Mann RS, Bruno RM, Hillman EM. Swept confocally-aligned planar excitation (SCAPE) microscopy for high-speed volumetric imaging of behaving organisms. Nat Photonics. 2015;9:113.
54. Migliori M, Datta MS, Dupre C, Apak MC, Asano S, Gao R, Boyden ES, Hermanson O, Yuste R, Tomer R. Light sheet theta microscopy for rapid high-resolution imaging of large biological samples. BMC Biol. 2018;16:57.
55. Chang BJ, Meza VDP, Stelzer EH. csiLSFM combines light-sheet fluorescence microscopy and coherent structured illumination for a lateral resolution below 100 nm. Proc Natl Acad Sci. 2017;114(9):4869–74.
56. Pitrone PG, Schindelin J, Stuyvenberg L, Preibisch S, Weber M, Eliceiri KW, Huisken J, Tomancak P. OpenSPIM: an open-access light-sheet microscopy platform. Nat Methods. 2013;10:598.
57. Glaser AK, Reder NP, Chen Y, McCarty EF, Yin C, Wei L, Wang Y, True LD, Liu JT. Light-sheet microscopy for slide-free non-destructive pathology of large clinical specimens. Nat Biomed Eng. 2017;1:0084.
58. Azaripour A, Lagerweij T, Scharfbillig C, Jadczak AE, van der Swaan B, Molenaar M, van der Waal R, Kielbassa K, Tigchelaar W, Picavet DI, Jonker A, Hendrikx EML, Hira VVV, Khurshed M, Van Noorden CJF. Three-dimensional histochemistry and imaging of human gingiva. Sci Rep. 2018;8:1647.
59. Sangha GS, Hu B, Bolus D, Wang M, Skidmore SJ, Sholl AB, Brown JQ, Goergen CJ. Multi-modality photoacoustic tomography, ultrasound, and light sheet microscopy for volumetric tumor margin detection. In: Proceedings of SPIE, Multimodal Biomedical Imaging XIII 2018, vol 10487, p 104870D.
60. Johnson SB, Cureoglu S, O'Malley JT, Santi PA. Comparison of traditional histology and TSLIM optical sectioning of human temporal bones. Otol Neurotol. 2014;35(7):1145–9.
61. Abadie S, Jardet C, Colombelli J, Chaput B, David A, Grolleau JL, Bedos P, Lobjois V, Descargues P, Rouquette J. 3D imaging of cleared human skin biopsies using light-sheet microscopy: a new way to visualize in-depth skin structure. Skin Res Technol. 2018;24(2):294–303.
62. Richardson DS, Lichtman JW. Clarifying tissue clearing. Cell. 2015;162(2):246–57.
63. Silvestri L, Costantini I, Sacconi L, Pavone FS. Clearing of fixed tissue: a review from a microscopist's perspective. J. Biomed. Optics. 2016;21(8):081205.